COMBINATION OF DIFFERENT UNSTEADY QUANTITY MEASUREMENTS FOR GAS TURBINE BLADE FAULT DIAGNOSIS

ΕΥΡ. ΛΟΥΚΗΣ
P. WETTA
Κ. ΜΑΘΙΟΥΔΑΚΗΣ
ΑΘ. ΠΑΠΑΘΑΝΑΣΙΟΥ
Κ. ΠΑΠΑΗΛΙΟΥ

ASME PAPER 91-GT-201

THE AMERICAN SOCIETY OF MECHANICAL ENGINEERS
345 E. 47 St., New York, N.Y. 10017

91-GT-201

Combination of Different Unsteady Quantity Measurements for Gas Turbine Blade Fault Diagnosis

E. LOUKIS*, Research Assistant
P. WETTA**, Principal Engineer
K. MATHIOUDAKIS*, Lecturer
A. PAPATHANASIOU*, Research Associate
K. PAPAILIOU*, Professor

*Laboratory of Thermal Turbomachines
National Technical University of Athens

**METRAVIB RDS

ABSTRACT

The exploitation of different unsteady quantity measurements for identifying various blade faults is examined in this paper. Measurements of sound emission, casing vibration, shaft displacement and unsteady inner wall pressure are considered. It is demonstrated that particular measurements are sensitive to specific faults. The suitability of measuring each of the above physical quantities for tracing the existence of each kind of fault is discussed. The advantage of combining different measurements originates from the possibility of extending the fault repertory covered when only one particular quantity is considered . The data analysis techniques employed range from conventional signal processing to the derivation of acoustic images of the engine outer surface. Relative features of each technique, as to their effectiveness and level of intrusivity, are discussed.

1. *INTRODUCTION*

Current needs for efficient and reliable operation of Gas Turbine power plants have resulted in the rapid growth of Condition Monitoring Techniques. Techniques based upon vibration measurements have found a wide application, because of their capability to identify various mechanical faults.

A desirable feature of Monitoring Techniques is their capability of not only determining gross faults, but faults of minor extent as well. Some minor faults do not probably disturb engine operation significantly, but they can be the precursors of catastrophic failures. Blade damage of turbomachinery components represent a fault of this category. Blades are among the most sensitive components of an engine because of their high stresses and rotational velocities. A slightly damaged blade does not influence engine overall performance, but it can result in major damage if the fault grows so that the blade is lost. Blade problems are for this reason well recognized for being responsible for the highest percentage of engine failures, as for example discussed by Simmons and Smalley (1989), and Lifson et al, (1990).

Another important feature a Monitoring Technique should possess, is the capability of identifying different kinds of faults with high reliability and minimum false alarm rates. But the main problem is that the diagnostic performance of a transducer can vary highly for different fault categories,as has been stressed by Lifsits et al(1986). They recommend that the vibration transducer selection should be according to the kind of faults we are interested in. The use of more than one indicator to identify a number of defects may be therefore beneficial, due to the different sensitivity of each indicator to each particular fault, as discussed by Baines (1987).

Aspects related to the above mentioned features are addressed in the present paper. Various unsteady quantity measurements, namely internal aerodynamic pressure, casing vibration, sound and shaft displacement have been acquired from an industrial Gas Turbine operating with different situations of faulty blades. Processing these data leads to the derivation of "fault signatures" which can be utilized for their identification. The relative merits of using each kind of measurements are discussed with respect to their sensitivity to particular faults and therefore their suitability for detecting them. It is also shown that by applying advanced processing of the data, the diagnosis can reach a high detail as to the kind and location of a blade fault. This refers in particular to the technique applied on acoustic field date, named Acoustic Imaging, as will be discussed in the corresponding section.

2. *EXPERIMENTAL SET-UP,MEASUREMENT AND PROCESSING TECHNIQUES*

The present investigation was based upon measurements on an Industrial Gas Turbine into which different faults were introduced. The test engine was the RUSTON'S TORNADO, described by Wood(1981), Charchedi and Wood (1982). Measurements

Presented at the International Gas Turbine and Aeroengine Congress and Exposition
Orlando, FL June 3-6, 1991

were obtained at nominal speed (11085 rpm) and 100%,75%,50% and 25% load. All results presented in the following figures correspond to 100 per cent load, unless stated otherwise, but the conclusions have been drawn from the whole amount of data.

During the experimental campaign four categories of measurements were performed simultaneously:

a - unsteady internal wall pressure, with Kulite type fast response transducers (P1 to P5 on figure-1)

b - casing vibration, with accelerometers mounted at the outside compressor casing (A1 to A6 on figure-1)

c - shaft displacement at compressor bearings, with a Bently Nevada system.

d - sound pressure levels, with double-layer microphones (similar to usual acoustic intensity probes), arranged on a circular rig, as shown in figure 1.

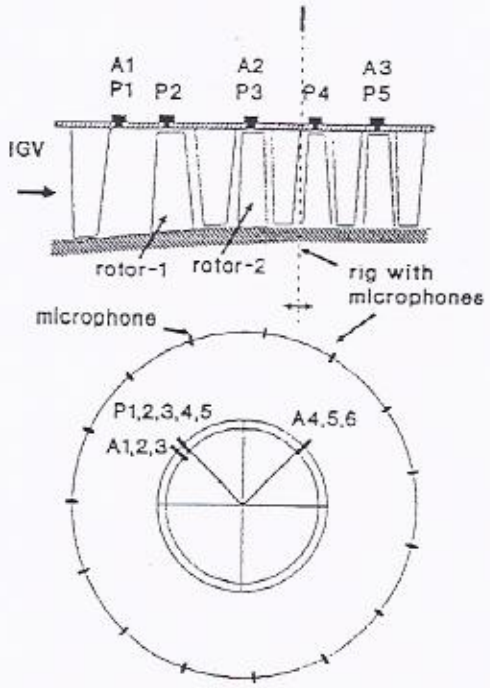

FIGURE 1. Schematic of instrument lay-out upon and around the compressor.

A schematic of the instrument placement is shown in figure 1. Internal pressure and casing acceleration measurements were acquired according to the description of Mathioudakis et al (1989a, 1990). The circular rig has 15 microphone pairs placed at equispaced angular positions. It was moved at ten positions along the Engine axis, and at each one of them rotated at ten equispaced circumferential positions, so that data from 150 circumferential locations were taken. Measurements were taken with a Data Acquisition System with a 32 channel, 960 Khz sampling rate capability.

Certain compressor blades were modified as shown schematically on figure 2, in order to simulate a number of realistic engine faults, according to the manufacturer's experience. Five experiments were performed testing the healthy engine datum and engines with the following four faults:

Fault-1. Rotor fouling; All stage-2 rotor blades were coated with textured paint in order to roughen blade surface and alter their contour,in order to simulate a fault of all the blades of only one rotor.

Fault-2. Individual rotor blade fouling; Two blades of stage-1 rotor separated by five intact blades, were coated by textured paint in order to simulate a slight individual rotor blade fault.

Fault-3. Individual rotor blade twisted ; A single blade of stage-1 rotor was twisted 8 degrees approximately in order to simulate a severe rotor blade fault.

Fault-4. Stator blade restaggering. Two stage-1 stator blades were mistuned in order to simulate a stator fault.

All subsequent numbered references to faults in the following text will correspond to the above classification.

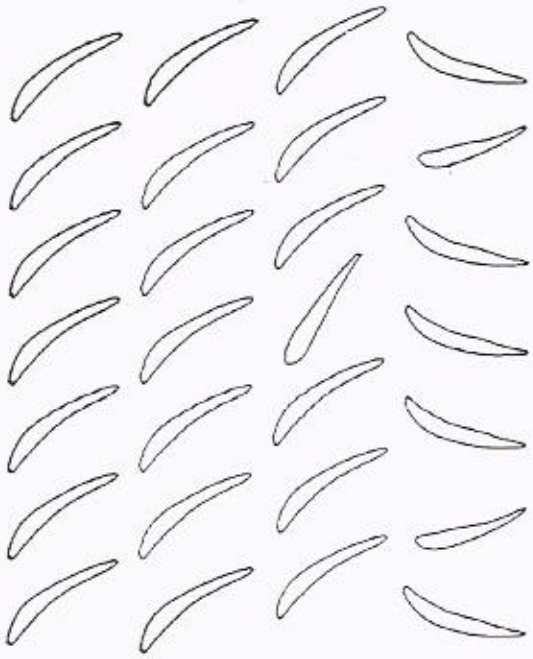

FIGURE 2. Schematic of investigated compressor faults.

The obtained measurements were divided in two groups: (i)The internal pressure, vibration, shaft displacement and one fixed location sound measurements. They will be referred to as point measurements and data from them were analyzed with spectral oriented methods. (ii)The double microphone array measurements. They will be referred to as acoustic field measurements, and their data were processed with spectral, cepstral and near field acoustic images techniques. Description of fault diagnosis possibilities for each group of measurements follows:

3. POINT MEASUREMENTS

3.1 Internal Unsteady Pressure Measurements

The suitability of internal unsteady pressure measurements for blade fault identification has

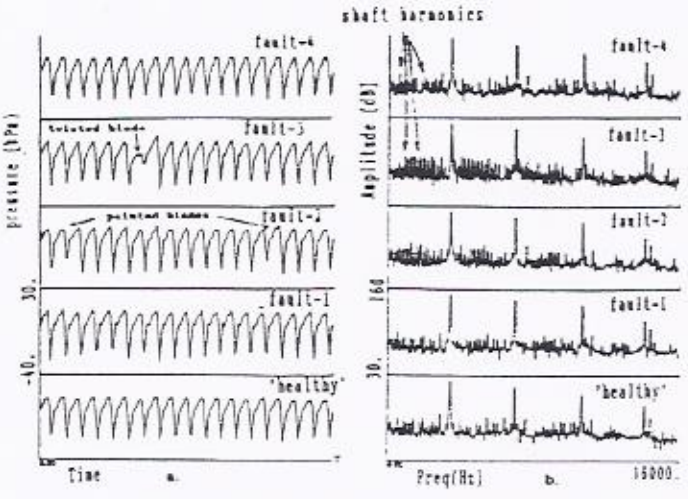

FIGURE 3. Pressure Transducer 2 (P2) signals for all tests; a.time traces b.spectra.

a[illegible]dy been presented by Mathioudakis et al ([illegible]). In the present paper a few additional data will be presented which complete the picture about pressure transducer capabilities, accompanying the properties of other instruments.

Phase averaged pressure time traces and the corresponding power spectra from the transducer of rotor-1 are shown in figure-3. On the time traces a marked difference can be seen only for the case of a twisted blade. The spectra for the same transducer show a distinct change through an increase of shaft harmonics for faults 2 and 3 and also smaller changes of poorly organized form for faults 1 and 4. On the other hand, observing similar data for pressure transducer of rotor 3, on figure 4, one can see that time traces are not identical, but it seems difficult to separate some well organized changes. Spectra show the emergence of some shaft harmonics, but again no organized pattern can be detected by visual inspection.

Analysis of results from the other pressure transducers downstream has shown that the presence of the faults is felt according to the location of the transducer relatively to the faulty rotor, and

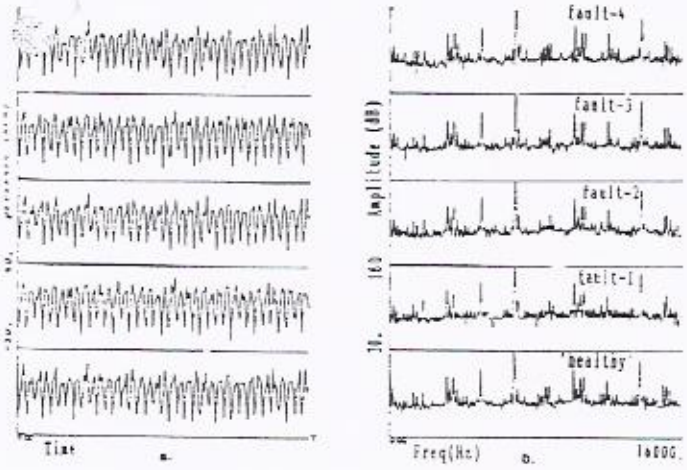

FIGURE 4. Pressure Transducer 4 (P4) signals for all tests; a.time traces b.spectra.

that clearly visible changes can be observed only for the transducer facing the rotor with the faulty blades. More details about the fault identification from data captured on such a rotor have been discussed in a previous work (Mathioudakis et al 1990).

3.2 Accelerometer Measurements

The signals of accelerometers located on the outer surface of the casing according to figure 1, are influenced not only by the closest compressor stage, but also by a number of neighbouring ones (Mathioudakis et al,1989a). So a rotating or stationary blading fault of a specific stage is expected to be sensed to a certain degree by all accelerometers.

The phase-averaged time domain signal of accelerometer A1, which is located in front of the first stage rotor, is shown in fig.5a for the five experiments. It can be noticed that all four faults cause certain differentiations mainly to the peaks and valleys of the signal. Specifically for Fault-4, which causes the highest differentiation, an increase of the signal amplitude can be observed. The corresponding spectra of accelerometer A1, are depicted on figure 5b for the 5 experiments. Again it can be noticed that all the four faults produce differentiations to the amplitude of the spectrum at various frequencies, mainly at the harmonics of the shaft rotating frequency. Also Fault-4 causes a significant increase to the first rotor blade passing frequency.

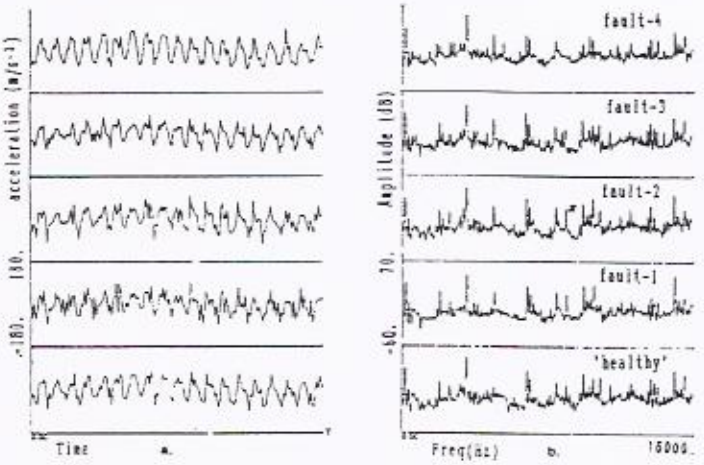

FIGURE 5. Accelerometer 1 (A1) signals for all tests; a.time traces b.spectra.

In fig.6 the signals of accelerometer A4 are shown. All four faults produce some differentiations to the amplitude of the spectrum mainly at the harmonics of the shaft rotating frequency with the most significant occurring at fault-4.

By examining both the phase-averaged time domain signals and the spectra of all the 6 accelerometers the conclusion which can be drawn is that all four faults produce some differentiations to the signals of the accelerometers. This holds to the same extent both for accelerometers axially located along the stage where the fault exists and for accelerometers located along a neighboring stage. The highest differentiation is

caused by Fault-4, which is associated with stationary blading, because of its mechanical connection to the casing.

Therefore, the accelerometers are sensitive to stationary blading faults, but also show some lower sensitivity to rotating blade faults of axially neighboring rotors.

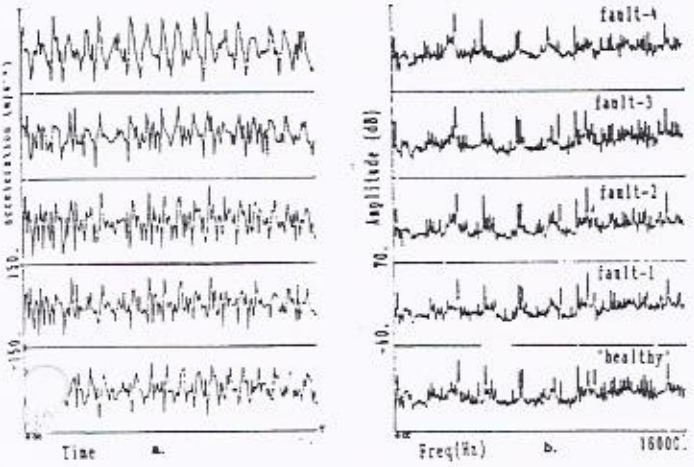

FIGURE 6. Accelerometer 4 (A4) signals for all tests; a.time traces b.spectra.

3.3 Shaft Displacement Measurements

The shaft displacement phase-averaged time domain signals, measured at the compressor bearings, are shown in fig.7a for the 5 experiments, while in fig.7b one can see the corresponding spectra. From these two figures it can be concluded that the healthy signal is close to a sinusoid with the shaft rotating frequency, and that the contribution of higher harmonics is much lower than the fundamental. The three rotor blade faults do not seem to produce any differentiation to the signal, while the stationary blading fault produces a small alteration, which can be observed in both time and frequency domain. This is due to the mechanical connection between the stationary blading of the compressor casing and the inlet section where the bearing housing is located.

It can be stated, conclusively, that the shaft displacement signal is not noticeably affected by the rotating blade faults, and shows a small sensitivity to the stator blading fault.

3.4 Single Microphone Measurements

Time traces and spectra from a single microphone are shown in figure 8. Both time traces and spectra show a distinct change for fault-4. It is observed that the spectrum exhibits a characteristic form developing a significant increase around the rotational harmonic of the first rotor. This is indicating that measurement by one single microphone can provide a clearly visible signature of stator faults.

This measurement cannot however provide an indication about the actual circumferential location of the fault, namely the angular location of the mistuned stationary blade. This is achieved by the derivation of acoustic images of the compressor outer casing as discussed in section 5.

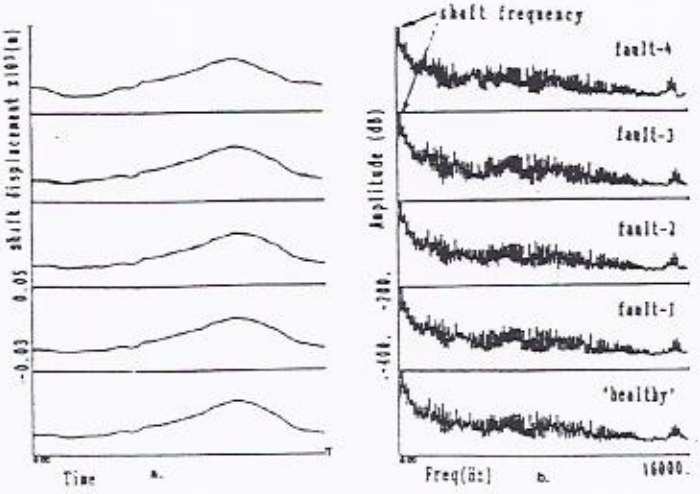

FIGURE 7. Shaft displacement sensor signals for all tests; a.time traces b.spectra.

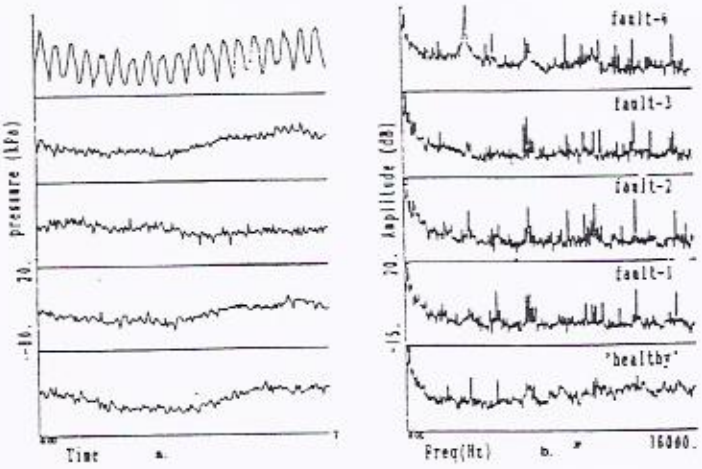

FIGURE 8. Microphone signals for all tests; a.time traces b.spectra.

4. DIFFERENCE PATTERNS

From the measurement results presented above, it can be stated that the fault diagnosis could be based upon the inspection of the signals. In some cases clearly visible alterations were noticed, but in many other cases there are differences which are minor and not well organized. For this reason the power spectra from the various instruments were further processed in order to extract more information about differences caused by implanted faults. The difference pattern of each fault, being an expression of its signature, was estimated by calculating the difference of the amplitude logarithms of spectra from intact and faulty machines. The following paragraphs describe part of an effort under way to classify the fault signatures and lays the foundations for a fault detection system.

The difference patterns of the unsteady pressure transducer 2 facing stage-1 rotor, produced by the 4 faults are shown in fig.9a. It can be observed that the difference patterns of faults 2 and 3, are of high magnitude. These two patterns

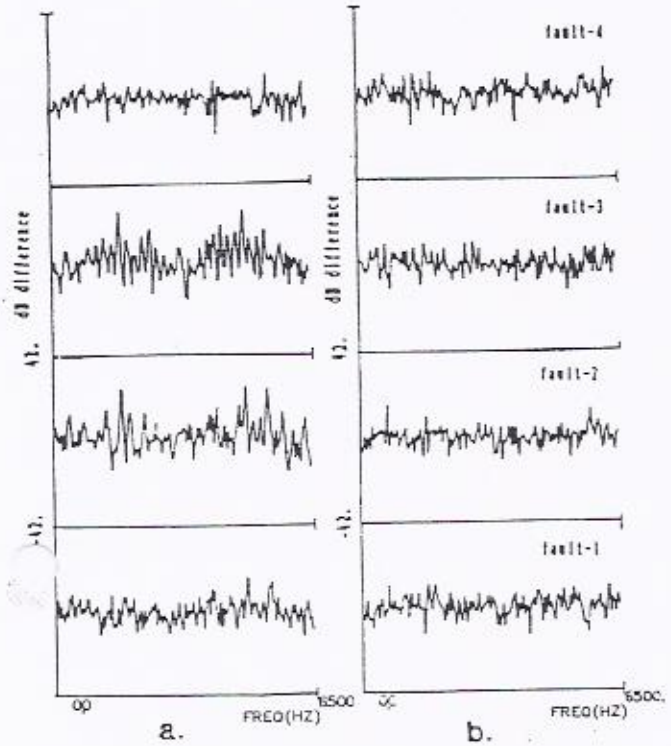

FIGURE 9. Difference patterns for all faults from: a.pressure transducer 2(P2) b.pressure transducer 4(P4)

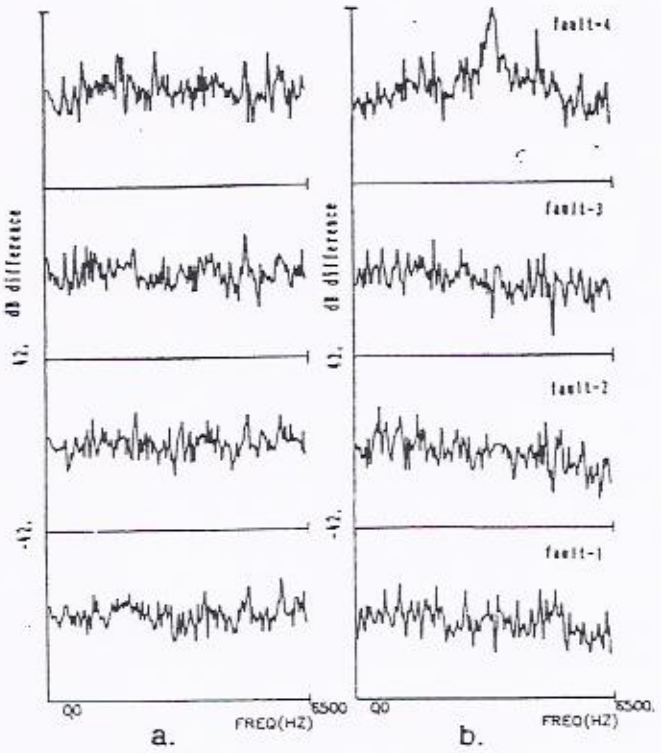

FIGURE 10. Difference patterns for all faults from: a.accelerometer 1(A1) b.microphone.

have their highest values at the rotational harmonics. On the other hand even for the faults 1 and 4, which produce, as observed in section 3.1, lower and not very clear differentiations, one can see that lower magnitude difference patterns are formed. Another useful remark is that the four difference patterns have different forms. Therefore the capability of distinguishing between the faults, from the corresponding difference patterns exists.

From fig.9b it can be stated that lower ampli- difference patterns are produced by the four .ts on the data of pressure transducer 4 facing age-3 rotor.

The same procedure was repeated for the other instruments as well. The four difference patterns of the accelerometer 1 at stage 2, are shown in figure 10a. Here, Fault-4 produces the highest magnitude difference patterns, in agreement with section 3.2. The 4 difference patterns vary in form,providing the capability of distinguishing between faults. The same trend was found when examining the rest of the accelerometers mounted on the compressor casing.

Finally referring to the single microphone signal, the four difference patterns are shown in figure 10b. Faults 3 and 4 correspond to higher magnitude patterns. The difference pattern of Fault-4 has a very high peak of the blade passing frequency of rotor, in agreement with section 3.4. The observation that the 4 patterns differ from each other substantially, holds for the single microphone as well.

The same patterns were calculated for the shaft displacement signal. They all were of very low magnitude, except the one of Fault-4 at the blade passing frequency of the first rotor where there is a peak, in agreement with section 3.3.

From the difference patterns which have been examined it can be stated that they are very sensitive to the differentiations caused by the various faults. For some cases of instruments, high and clearly visible spectra alterations have been observed, but for other cases of lower and less clear ones.

The calculation of difference patterns have shown that they exhibit two properties which make them suitable as fault signatures:
(a) for each instrument, different faults produce different patterns
(b) the pattern of each fault is repeatable for different tests at different engine loads. The data backing this second conclusion are not presented in this paper, due to space limitations but similar data have been presented by Mathioudakis et al (1990).
The above two properties indicate that spectral difference patterns are a useful tool for the analysis of the differentiation caused to various instruments signals by existing faults, and also for the implementation of a diagnostic system for blading faults.

5. ACOUSTIC FIELDS PROCESSING

A second class of methods considered here for producing diagnostic information are methods based on the double microphone scanning data. Such a technique is the Acoustic Imaging Technique, described by Wetta et al (1988).

The main advantage offered by processing the acoustic field measurements with the nearfield

acoustic imaging techniques, is to minimize:
i) The influence of other sound sources in the vicinity of the engine
ii)The influence of reflected and scattered sound by surrounding surfaces.
These problems are expected to exist in an industrial environment, and can lead to wrong conclusions if they are not dealt with.

Another ability of these techniques (Gaudriot,L.,et al, 1980; Maynard,J.D.,et al, 1985) is the determination of the sound sources location from the nearfield acoustic measurements. This capability is very useful from the diagnostic point of view, because it can provide additional information on the location of the fault, which cannot be derived from the time and frequency domain analysis of point measurements.

The results of the technique can be used to elaborate discriminant functions, sensitive to the investigated faults, as described by Wetta (1990). Three types of discriminant function analyzing various patterns are adopted.

a) A spectral discriminant function, defined as the total acoustic power $P_a(f)$ which is radiated by a given part of the gas turbine (e.g. compressor component in our case). It is obtained by spatial integration of the normal component of the intensity vector on the whole double-layer cylindrical array of microphones ,which surrounds the compressor casing.

b) A pseudo-temporal discriminant function, named acoustic power Cepstrum function $C_p(r)$, which is obtained by inverse Fourier transform of the logarithm of the previously defined acoustic power spectrum:

$$C_p(r) = F^{-1}\,[P_a(f)].$$

This kind of processing, applied on the total acoustic energy emitted by the compressor component, allows to exhibit more accurately (with a high signal/noise ratio) the effect of a periodic fault.

c) A spatial discriminant function , defined as the acoustic pressure distribution on the compressor casing. It is determined by processing the acoustic field measurements from the acoustic array by the Acoustic Imaging Beckpropagation methods (Wetta et Al, 1989). ; ;This allows to obtain at a given frequency f e spatial signature close to the sources mechanisms in order to precisely localize them, as well as to determine the nature of sources fields on the casing (e.g. extended waves, localized sources)

When applied to the RUSTON'S TORNADO and for the various investigated blade fault configurations, the above processing has led to the results presented in the following sections:

5.1 Acoustic Power Spectrum Calculations (spectral patterns)

The most characteristic pattern is obtained for Fault-4 ,whose spectrum is shown in fig.11. We can notice, comparing with the corresponding healthy spectrum, that the peak around the rotational harmonic nº 19 (3510Hz blade passing frequency of rotor stage being just upstream to the faulty stator stage) becomes wider. There is also a great increase (+4dB) of the rotational harmonic nº 27 (4900Hz: blade passing frequency of rotor stage being just downstream the faulty stator stage).

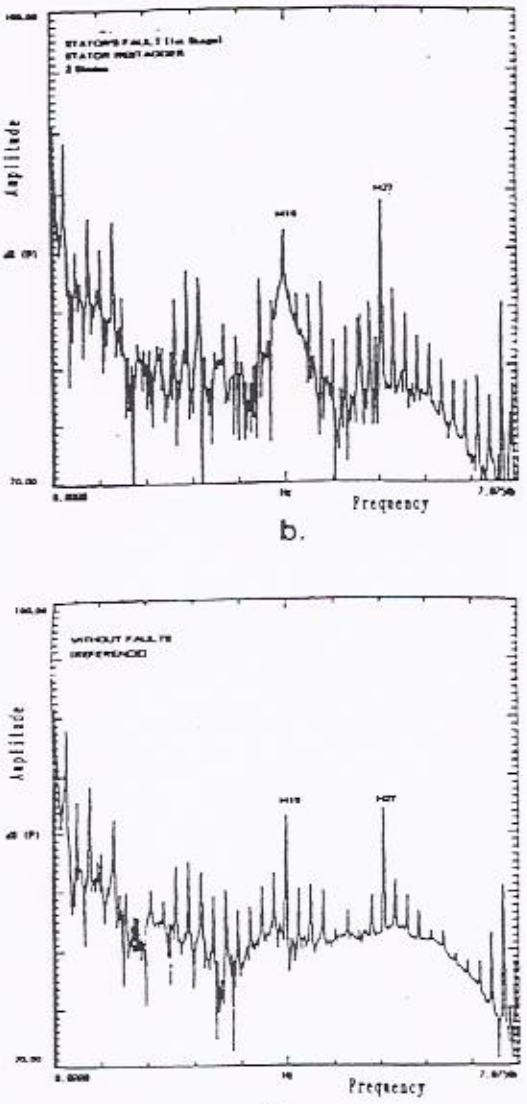

FIGURE 11. Acoustic Power Specrum for: a. 'healthy' engine b. fault-4

Spectral patterns obtained for rotor faults 1,2,3 (not shown here) do not exhibit great specific variations of the peaks. Generally speaking, variations are very small (+2dB) and distributed over the whole set of multiple harmonics.

5.2 Acoustic Power Cepstrum Calculations (pseudo-temporal patterns)

Examination of acoustic power Cepstrum indicates that,in general, high Cepstral values are obtained for the periods
T=1T,2T,3T,4T with T= period of rotation as can seen in figure 12 for the case of the twisted blade.

The observed variations for T = 1T with respect to the corresponding value on the reference Cepstrum (healthy condition) are the following: +15.7% for Fault-1 , +8.9% for the Fault-2 , +56.35% for the Fault-3 and 48.15% for the Fault-4. These alterations are then significant ,even for rotor faults, taking into account the stability of cepstra values that characterizes a healthy engine.

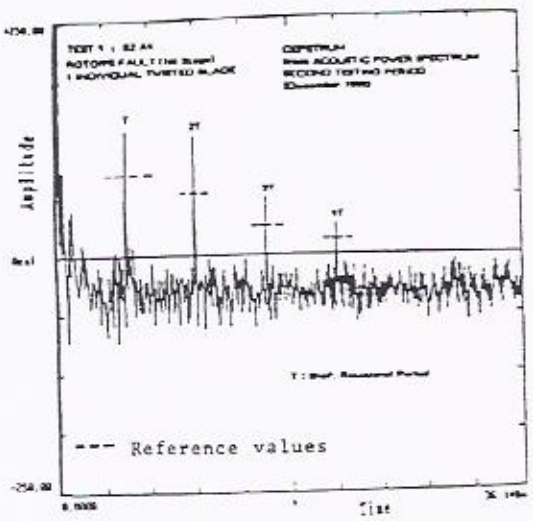

FIGURE 12. Acoustic Power Cepstrum for fault-3

3 Backpropagated images (spatial patterns)

The most interesting spatial patterns are again obtained for the stator fault and more particularly for harmonics nº 19 and nº 27 (first and second blade passing frequencies).

Specifically for the stator fault and harmonic nº 19, the array image,corresponding to the acoustic pressure distribution on the measurements cylindrical surface,is shown in fig.13. The backpropagated image, corresponding to the acoustic pressure distribution on the compressor casing,is shown in fig.13b.It exhibits high values of acoustic pressure ,which are very well circumferentially localized , and correspond exactly to the angular positions of the mistuned vanes of stator 1.Therefore this technique enables the detection of the circumferential position of the mistuned blades

Concerning spatial acoustic patterns obtained for the rotor faults, no significant or clear variations can however be observed for any studied harmonic.

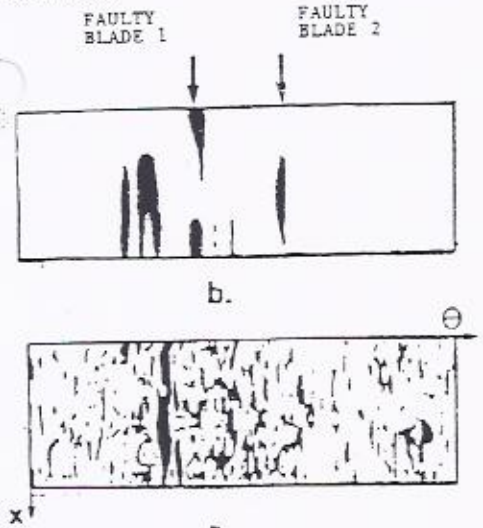

FIGURE 13. Acoustic imaging pressure (first blade passing harmonic) field on: a. array surface b.compressor casing surface.

6. CONCLUSIONS

A comparative study of the possibility to detect the presence of blade faults in a Gas Turbine compressor by exploiting various unsteady quantities' measurements has been presented.It was found that different instruments and measurements are more suitable than others for each particular fault.

For the spectral oriented fault detection techniques concerning the instruments mounted on the engine and a single microphone, the following conclusions can be drawn:

- rotor blade faults are best identifiable by a pressure transducer facing the rotor
- pressure transducers located at neighboring rotors also sense a differentiation, but the patterns are not as clearly identifiable by visual inspection
- accelerometers sense a differentiation, the magnitude of which depends on the location of accelerometer on the casing. The differentiation patterns exhibit les. well organized form than the pressure transducer on the corresponding rotor
- no visually observable changes on shaft displacement measurement results were remarked.
- stator blade faults produced a distinct signature both on accelerometer and a single microphone measurement results

Three major features of acoustic imaging techniques lead to the following conclusions:

- Acoustic Power Cepstrum calculations allow the detection of the presence of a blade fault, both rotor and stator ones.
- Acoustic power Spectrum calculations allow the diagnosis of a stator fault, as well to localize it axially, in the extent that the effects are observed on blade passing frequencies of a stage.
- Backpropagated imaging allows the diagnosis of a stator fault as well as the precise localization of the angular positions of the faulty vanes. It is expected in the future to adapt this backpropagation technique to the analysis of moving sources, which will lead to the capability of localizing rotor faults as well.

7. REFERENCES

Baines N.,1987, "Modern Vibration Analysis in Condition Monitoring.Noise and Vibration Control Worldwide", May 1987, pp 148-151.

Carchedi,F.,and Wood,G.R.,1982,"Design and Development of a 12:1 Pressure Ratio Compressor for the Ruston 6-Mw Gas Turbine", ASME Paper No 82-GT-20.

Gaudriot,L.,Mercusot,M.,and Escudie,B.,1980,"Near and far field techniques in analysis of noise radiation mechanism", Revue d' Acoustique nº 54, 1980, pp 176-189.

Lifsits A.,Simmons A.,and Smalley A.,1986. "More Comprehensive Vibration Limits of Rotating Machinery", Journal of Engineering for Gas Turbines and Power, Vol 108, Oct 1988, pp 583-590.

Lifson A., Smalley A., Quentin G., and Zanyk J., 1990, "Assessing Diagnostic Techniques for Problem Identification in Advanced Industrial Gas Turbines", Paper ASME 90-GT-365, 35th Gas Turbine and Aeroengine Congress, June 11-14, 1990.